Experimental evaluation of hollow-core wall orientation in steel moment frame

Mehdi Nazarpour, Parsa Monfaredi, and Abdoreza S. Moghadam

- This paper describes the experimental program designed to evaluate the seismic performance of hollow-core wall units in steel moment frames.
- Two half-scale specimens were constructed with hollow-core wall panels placed either vertically or horizontally in a steel moment frame to investigate the effect of panel orientation on the seismic performance of the wall system.
- The results of the lateral load testing indicated that the vertical placement of hollow-core wall units controlled nonstructural damage, improved the seismic behavior of the steel moment frame, and resisted higher lateral loads than the horizontally placed hollow-core wall units.

PCI Journal (ISSN 0887-9672) V. 64, No. 3, May–June 2019.
PCI Journal is published bimonthly by the Precast/Prestressed Concrete Institute, 200 W. Adams St., Suite 2100, Chicago, IL 60606.

Hollow-core panels used as precast concrete wall units are a common building component, especially in steel structures. These precast concrete walls offer several advantages compared with traditional concrete or masonry walls, such as improved economy, better out-of-plane behavior, labor savings, and easy and fast finishing.[1] In addition, hollow-core units used as exterior walls below the finished ground level in steel buildings, where they resist soil pressure, are beneficial and cost effective.

Although life safety design criteria permit some damage under seismic loading, nonstructural component damage is one of the main causes of death in an earthquake.[2] Thus, reducing the damage caused by infilled frames is important. Furthermore, it is desirable to use nonstructural walls that can improve seismic behavior of structures instead of traditional infilled frames.[2]

The most common nonstructural walls are unreinforced masonry infills provided in steel frame panels.[1] Unreinforced masonry infills are constructed after the steel frame is in place. However, hollow-core wall panels are placed at the same time as the steel frame columns, after which the upper beam is connected to complete the frame.

There is significant uncertainty regarding the behavior, failure modes, and energy-dissipation capacities of hollow-core infill panels in steel frames under earthquake loading. At present, there are no specific provisions for hollow-core panel orientation in steel moment frames, and the orientation

that enables the most effective performance and least damage is unknown. A lack of adequate testing contributes to this uncertainty. The behavior of hollow-core wall panels under seismic loading is especially important when considering the impact of nonstructural damage.

The design specifications that are available for hollow-core units mainly discuss their use as slabs.[3–7] Many studies have been carried out to evaluate the structural behavior of these slabs.[8–15]

Previous studies demonstrated that if the connection details are modified, single hollow-core walls are capable of resisting substantial lateral loads despite their lack of transverse shear reinforcement.[2] However, a study on a single wall panel alone is insufficient to assess the overall structure performance under earthquake loads.

The seismic design of precast concrete walls with additional details, such as shear connectors and spiral reinforcement, are presented by Perez et al.,[16] and the seismic performance of precast concrete walls with armoring details based on rocking behavior are discussed by Holden et al.[17]

The authors' research shows that there is no other experimental study that examines the multipanel hollow-core walls under lateral loading without any modification to their details, such as connectors and energy dissipators. In addition, there is little information about the seismic behavior of these infill panels in steel moment frames.

Hamid and Mander's study[1] indicates that a multipanel wall system consisting of seismic and nonseismic wall panels, which are designed to rock on their foundations can be used in high seismic regions. The panels used in the study included fused bars, rubber seating pads, silicone sealant, rubber block spacers, and other details.

Hollow-core units are precast concrete panels with two layers of high-strength, bonded pretensioning strands constructed with high-strength, low-slump concrete. This paper examines the behavior of hollow-core units used as nonstructural partition walls to determine whether they enhance the seismic performance of steel frames.

The goal of this study was to evaluate the effect of the orientation of the hollow-core units and layers of strands on the performance of the system. The most desirable orientation would enhance the overall behavior of the steel moment frame and improve its performance under seismic loading conditions with minimal damage.

This paper presents experimental results that evaluate the seismic behavior of precast concrete hollow-core walls so that they can be modified, redesigned, and finally implemented in moderate to high seismic regions as structural walls in steel structures.

Experimental program

Specimens

The vertical panels used in this study were 880, 150, and 1260 mm (34.6, 6.0, and 49.6 in.) in length, thickness, and height, respectively, while the horizontal panels were 1760, 150, and 630 mm (69.3, 6.0, and 24.8 in.) in length, thickness, and height, respectively (**Fig. A.1**; for appendix figures, go to www.pci.org/2019May-Appx). The panels were placed in a vertical or horizontal orientation in two identical half-scale steel moment frames with rigid reduced-beam-section connections. In specimen HP-RC (horizontal panels in rigid connection frame), two hollow-core panels were placed horizontally, whereas specimen VP-RC (vertical panels in rigid connection frame) had two hollow-core panels placed vertically.

Box section steel columns and built-up steel plate beams were constructed by a steel fabricator and then assembled into a frame with the hollow-core panels. Longitudinal fillet welds joined four steel plates to form the steel box columns (Fig. A.1).

It should be noted that, according to the American Institute of Steel Construction's *Prequalified Connections for Special and Intermediate Steel Moment Frames for Seismic Applications* (AISC 358-10),[18] in built-up box columns, flange and web plates of box columns shall be joined by complete-joint-penetration groove welds within a zone extending from 300 mm (12 in.) above the upper beam flange to 300 mm below the lower beam flange. But for this study, fillet welds were specifically chosen for the beam-column joints to analyze the behavior of the beam-column connection. Figure A.1 shows the details and dimensions of both specimens' components.

Materials

The properties of the structural steel and the concrete compressive strength were determined using ASTM E8/E8M[19] and ASTM C39/C39M[20] standard tests, respectively. ASTM A416/A416M[21] testing was performed on the strands. Details of the material properties are summarized in **Table 1**.

Table 1. Material properties

Steel	Concrete	Strand
F_y = 273 MPa	f'_c = 58 MPa	Seven-wire steel strand
F_u = 356 MPa	w/c = 0.4	1860 MPa Grade LR ASTM A416
E = 231.139 GPa	Weight = 2403 kg/m^3	Diameter = 9.5 mm

Note: E = modulus of elasticity of steel; f'_c = concrete compressive strength; F_u = ultimate tensile strength of steel; F_y = yield strength of steel; LR = low relaxation; w/c = water-cement ratio. 1 mm = 0.0394 in.; 1 MPa = 0.145 ksi; 1 GPa = 145 ksi; 1 kg/m^3 = 1.6875 lb/yd^3.

Test setup and instrumentation

Figure 1 shows the schematic arrangement of the experimental setup with an in-plane actuator attached to the reaction frame. Each column was fixed to the reaction frame by eight anchored bolts. Lateral load was applied by a 1000 kN (225 kip) actuator, and the force was measured by an in-series load cell. Each specimen was loaded laterally with forces applied through the loading beam, which was a stiffened 220 mm (8.7 in.) deep European wide-flange beam (IPB 220). A quasi-static cyclic reversed lateral force was applied at the center of the loading beam, which was located 1945 mm (76.6 in.) above the reaction frame.

Figure 2 shows the test setup. A constant low axial load was applied to the specimens by circular solid steel rods. The axial compression load in each column was 80 kN (18 kip). In addition, four 160 mm (6.3 in.) deep channel bars were attached to the beams and columns to prevent out-of-plane movement of the panels.

The experiments were conducted in drift control. The drift ratio was calculated by dividing the difference between the displacement of the top and bottom of the steel moment frame by the column height. During the test, lateral displacements were recorded using linear variable displacement transducers (LVDTs). **Figure A.2** shows the position of the LVDTs. Image processing techniques were used to determine the overall deformation of the frames and the grid points on the panels.

The loading procedure was limited by the range of amplitude of the hydraulic actuator, which was 120 mm (4.7 in.) in the positive direction (pulling) and 120 mm in the negative direction (pushing). Therefore, the applied displacements were the same for corresponding cycle numbers for both specimens, but the applied load was variable. In other words, both loading tests were stopped at the maximum possible displacement of the hydraulic actuator, which corresponded to an ultimate drift ratio of 8.3%.

Loading history

The nominal loading history suggested by the Federal Emergency Management Agency's (FEMA's) *Interim Testing Protocols for Determining the Seismic Performance Characteristics of Structural and Nonstructural Components*[22] was used to test the two specimens described in this paper. Each complete load cycle consisted of one half cycle in the positive direction and one half cycle in the negative direction (Fig. 1). **Figure 3** shows the loading history of the test program.

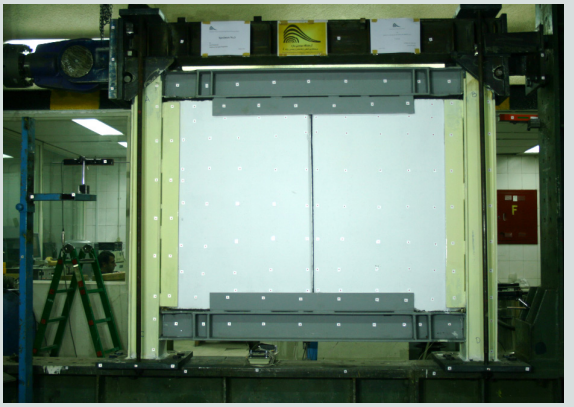

Figure 2. Photograph of experimental setup.

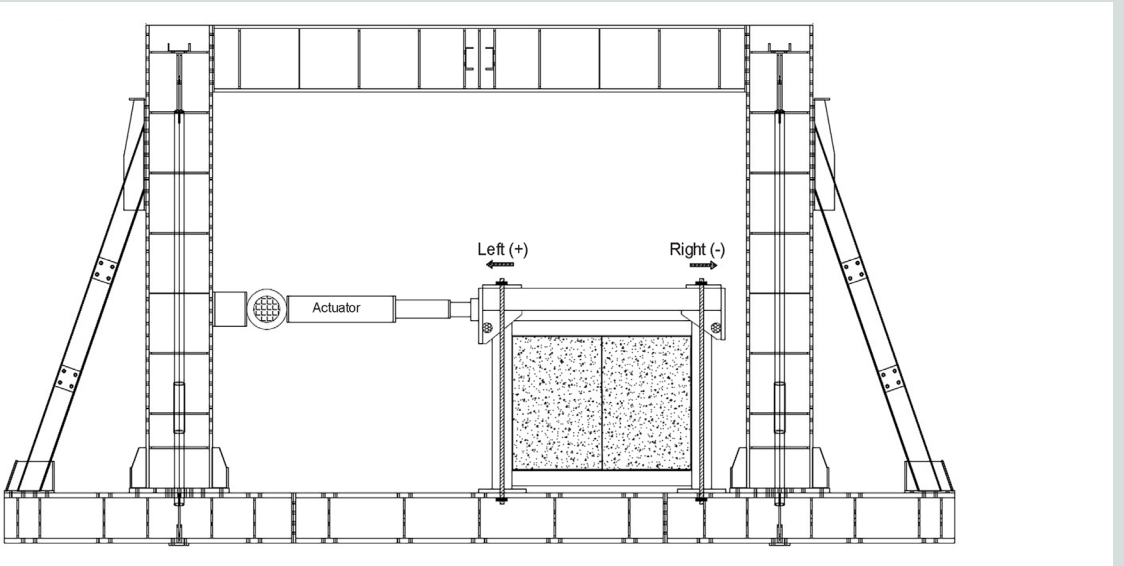

Figure 1. Schematic arrangement of experimental setup for specimen with vertical panels in rigid connection frame. Note: IPB 220 = 220 mm (8.7 in.) deep European wide flange beam.

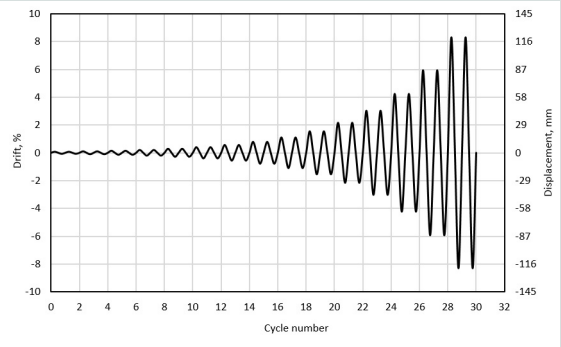

Figure 3. Loading history for experimental program. Note: 1 mm = 0.0394 in.

Test results and discussion

Behavior of specimens

Figure 4 shows that two distinct responses to lateral load were observed. In HP-RC, the horizontal panels slid against each other; while in VP-RC, the two wall units rocked laterally within the steel moment frame.

In the last testing cycle, the maximum movement of the two horizontal panels against each other was determined to be 65 mm (2.6 in.) using image processing techniques. In VP-RC, the maximum movement of the panels was 15 and 95 mm (0.6 and 3.7 in.) in the horizontal and vertical directions, respectively. Figure 4 shows the shape of the gaps between the panels and columns. Due to these gaps, the pinching in hysteresis behavior of VP-RC was predictable. The independent rocking behavior and the formation of compression struts on each vertical panel led to a significant increase in the total stiffness of the system, which increased the load threshold of the vertical panels compared with the horizontal panels.

Hysteresis curves

Figure 5 shows continuous plots of applied lateral load compared with the drift ratio for specimens HP-RC and VP-RC. The difference in the applied lateral load at the same drift ratios for the frame with vertical hollow-core panels and the frame with horizontal hollow-core panels can be seen by comparing the two plots.

At the ultimate drift ratio (8.3%), specimen VP-RC with vertically oriented hollow-core walls resisted approximately 15% higher loads than specimen HP-RC.

Table 2 shows the overall response of the specimens, including peak loads corresponding to the ultimate drift ratio.

Modes of failure

In Fig. 5, letters shown in each graph correspond to the failure

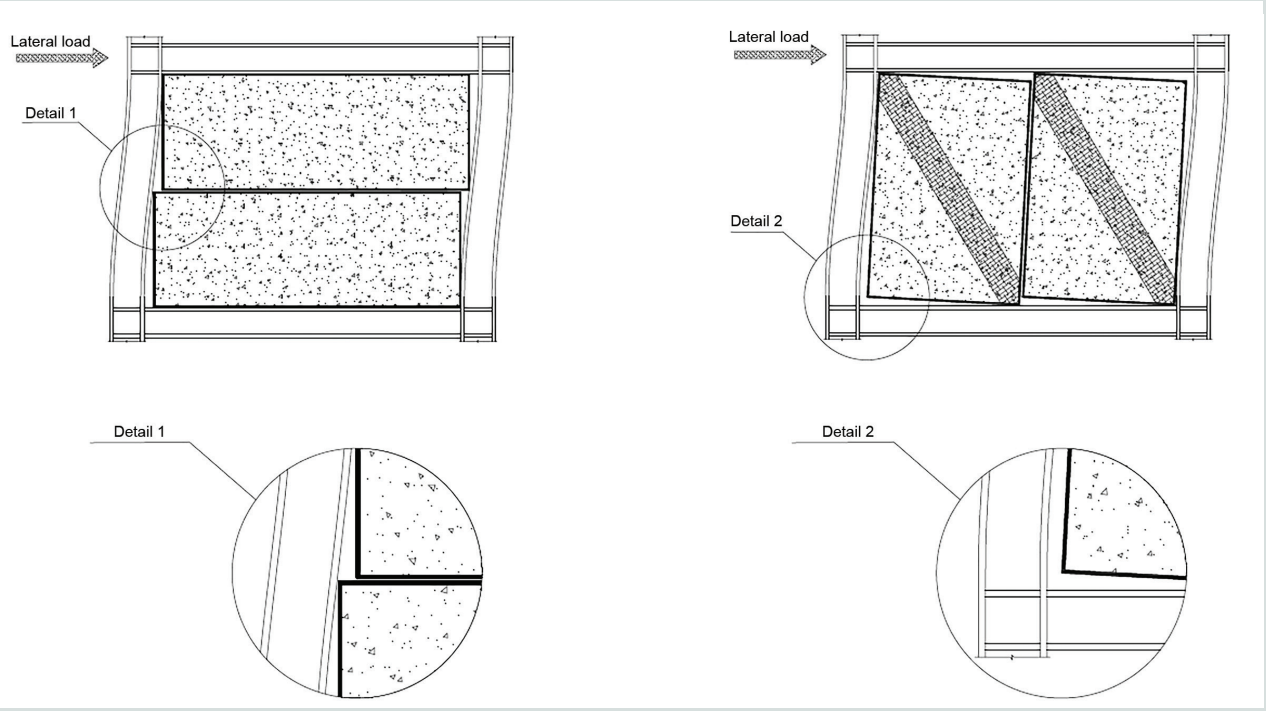

Specimen with horizontal panels in rigid connection frame

Specimen with vertical panels in rigid connection frame

Figure 4. Hollow-core wall specimen responses to lateral load.

Table 2. Peak loads and measured drift ratios for specimens HP-RC and VP-RC

Specimen	Peak load, kN	Drift ratio, %
HP-RC	538	7.7
	–623	–8.3
VP-RC	658	8.3
	–735	–5.9

Note: HP-RC = horizontal panels in rigid connection frame; VP-RC = vertical panels in rigid connection frame. 1 kN = 0.225 kip.

modes. The sequence of letters follows the order in which each failure occurred during the test. The test results show that at the ultimate drift ratio, the hollow-core panels in VP-RC had more damage than the panels in HP-RC, while the steel frame of VP-RC had less damage than the steel frame

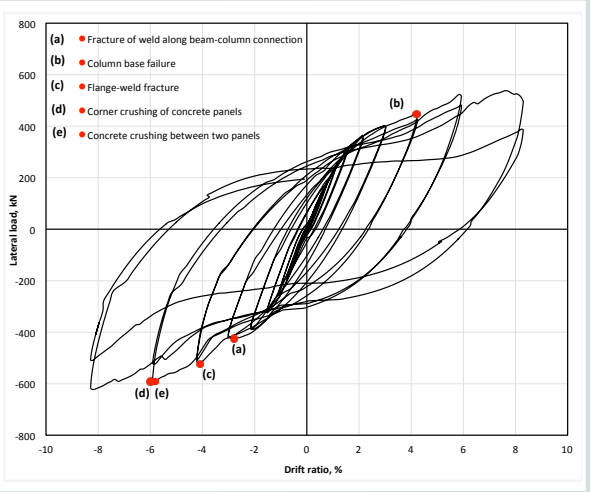

Specimen HP-RC

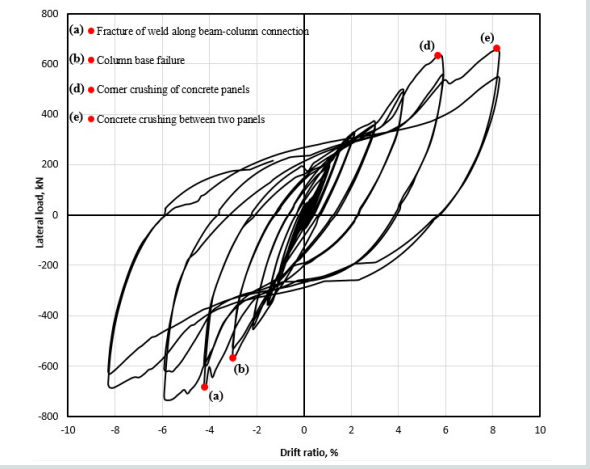

Specimen VP-RC

Figure 5. Experimental hysteresis curves for specimens. Note: HP-RC = horizontal panels in rigid connection frame; VP-RC = vertical panels in rigid connection frame. 1 kN = 0.225 kip.

of HP-RC. VP-RC resisted higher loads at the ultimate drift ratio and had a greater chance of additional load resistance compared with HP-RC, but the range of the hydraulic actuator limited the ultimate drift ratio, and the testing had to be stopped before the ultimate load resistance was reached.

Figures 6 and **7** show the observed failure modes for each specimen. Each failure mode is referred to using the same notation shown in the hysteresis curves of Fig. 5.

One desirable goal is to postpone and reduce the damage

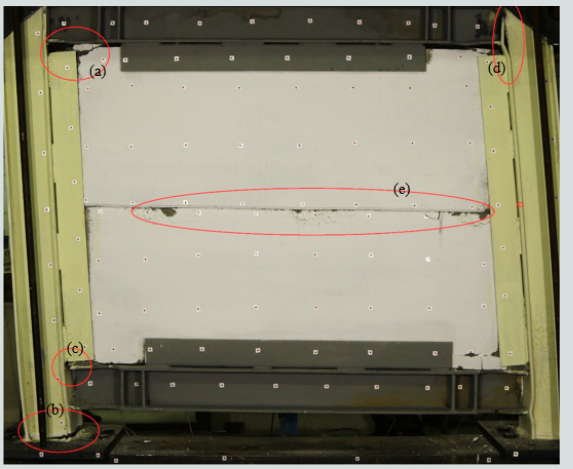

Figure 6. Observed failure modes and damage for specimen with horizontal panels in rigid connection frame. Note: (a) = fracture of weld along beam-column connection; (b) = column base connection failure; (c) = flange-weld fracture; (d) = corner crushing of concrete panels; (e) = concrete crushing between two panels.

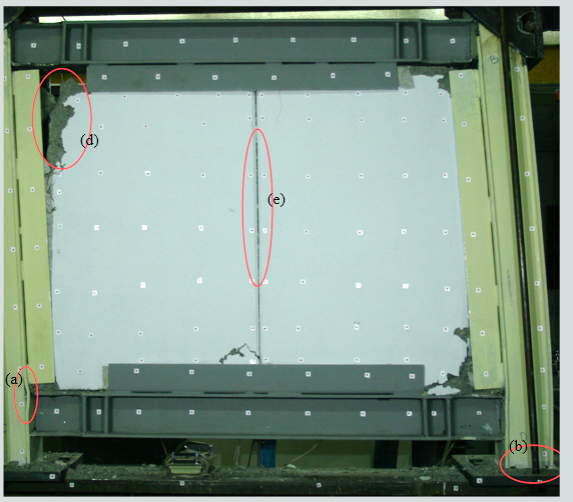

Figure 7. Observed failure modes and damage for specimen with vertical panels in rigid connection frame. Note: (a) = fracture of weld along beam-column connection; (b) = column base connection failure; (d) = corner crushing of concrete panels; (e) = concrete crushing between two panels.

to the structural members simultaneously by transferring the damage from the steel frames (structural elements) to the hollow-core panels (nonstructural elements). Thus, all damage and failure modes of the specimens were classified as either steel frame component failure modes or hollow-core panel failure modes. The main failure modes for steel frame components were fracture of the weld along the beam-column connection, column base connection failure, and fractures in the end of the beam-flange welded joint or the toe of the weld access hole. Failure modes for hollow-core panels were corner crushing of concrete panels and concrete crushing between two panels. **Table 3** provides a brief overview of all failure modes with their corresponding drift ratios and loading.

One of the main failure modes in HP-RC was failure of the beam-column joint that has emerged in flange-weld fracture. This is an undesirable failure mode that occurred due to local transition of lateral load to the joint, and it did not occur in VP-RC.

Failures in the beam-column joint observed in this experimental research emphasize the necessity for the provisions regarding built-up box columns presented in AISC 358-10.[18]

Idealized backbone curves

The backbone curve of hollow-core panels and steel moment frames provides information that is fundamental for their structural assessment. According to FEMA's *Improvement of Nonlinear Static Seismic Analysis Procedures*,[23] this curve corresponds to the envelope of the hysteresis loops obtained experimentally in walls subjected to in-plane cyclic loading. In this research, idealized backbone curves were derived from ASCE/SEI 41-13.[24] Because the experimental tests did not enter the degradation phase, the idealized curves are bilinear. **Figure 8**

Table 3. Summary of failure modes

Element	Failure mode	Specimen HP-RC		Specimen VP-RC	
		Load, kN	Drift ratio, %	Load, kN	Drift ratio, %
Steel frame	Fracture of weld along beam-column connection	–425	–2.8	–686	–4.2
	Column base connection failure	447	4.2	633	5.7
	Flange-weld fracture	–523	–4.1	n/a	n/a
Hollow-core wall panel	Corner crushing of concrete panels	–592	–5.9	–568	–3.0
	Concrete crushing between two panels	–592	–5.9	658	8.2

Note: HP-RC = horizontal panels in rigid connection frame; n/a = not applicable; VP-RC = vertical panels in rigid connection frame. 1 kN = 0.225 kip.

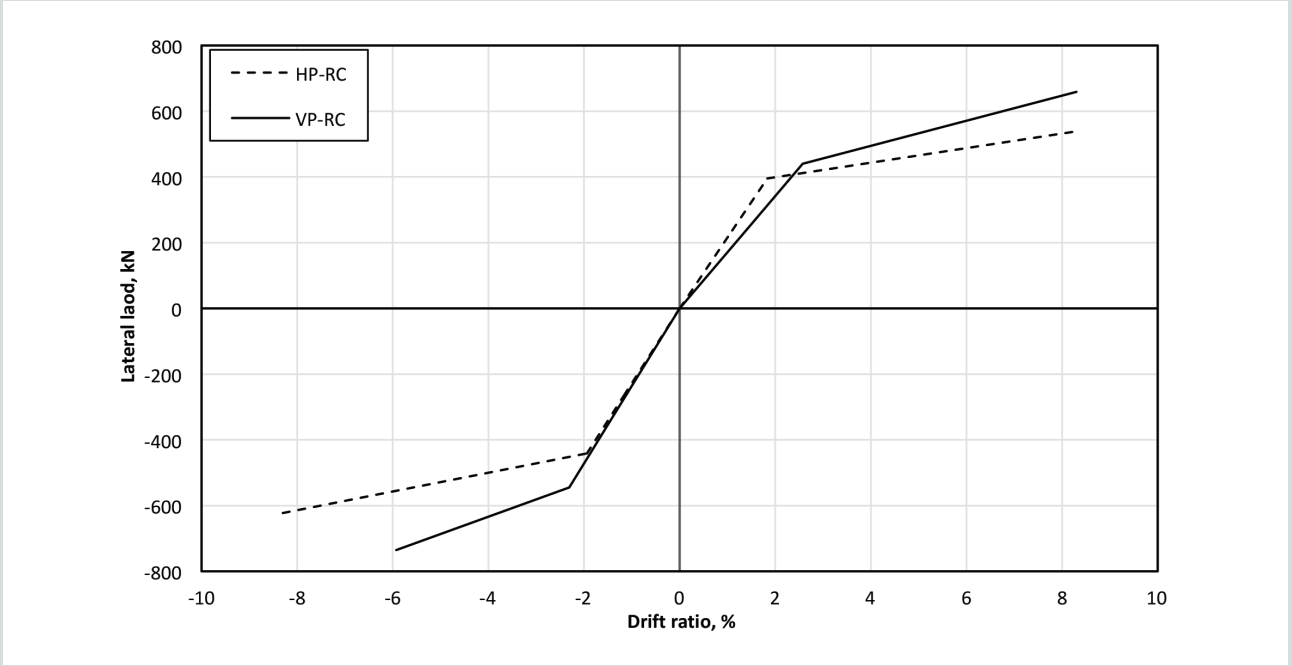

Figure 8. Idealized backbone curves. Note: HP-RC = horizontal panels in rigid connection frame; VP-RC = vertical panels in rigid connection frame. 1 kN = 0.225 kip.

Table 4. Key parameters of each specimen for idealized backbone curves

Specimen	K_e, kN/mm	V_y, kN	V_d, kN	Δ_y, mm	Δ_d, mm	δ_y, %	δ_d, %
HP-RC	14.9	396	538	26.6	120	1.8	8.3
	–15.7	–442	–623	–28.1	–120	–1.9	–8.3
VP-RC	11.8	440	658	37.2	120	2.6	8.3
	–16.3	–545	–735	–33.4	–85.8	–2.3	–5.9

Note: HP-RC = horizontal panels in rigid connection frame; K_e = effective lateral stiffness of the specimen; V_d = applied load at ultimate strength; VP-RC = vertical panels in rigid connection frame; V_y = applied load at yielding; δ_d = drift ratio at ultimate strength; δ_y = drift ratio at yielding; Δ_d = lateral displacement at ultimate strength; Δ_y = lateral displacement at yielding. 1 mm = 0.0394 in.; 1 kN = 0.225 kip; 1 kN/mm = 5.71 kip/in.

shows the bilinear idealization of the backbone response curves of the specimens.

Table 4 presents the key parameters used to derive the idealized backbone curves. The effective lateral stiffness K_e, load V, lateral displacement Δ, and drift ratio δ are shown for both positive and negative load. The subscript y refers to yielding point, and d refers to ultimate strength. Figure 8 shows that the strength of the specimens initially increases through hardening behavior, but ultimately strength and stiffness both degrade through softening behavior.

Stiffness-degrading behavior

The differences in construction methods between the steel moment frames with vertical hollow-core panels compared with the frames with horizontal hollow-core panels resulted in variations in seismic behavior.

The upper panel of specimen HP-RC was placed on the lower panel without any gap between panels, so they could easily slide against each other. A gap formed between the horizontal panels as the cyclic loading gradually increased.

Specimen VP-RC was constructed with a 15 mm (0.6 in.) gap between the vertical panel and columns, which caused the stiffness degradation at initial drift ratios for specimen VP-RC to be greater than for HP-RC. **Figure 9** shows that both specimens had similar stiffness values (13 kN/mm [74 kip/in.]) at a drift ratio of 2%. As the testing continued and loads increased, the initial gaps for specimen VP-RC gradually closed, which led VP-RC to ultimately have a stiffness that was up to 20% greater than the stiffness of HP-RC.

Comparing the stiffness degradation curves indicates that specimen VP-RC had larger reductions in stiffness than HP-RC had during reversed cyclic loading until 2% drift ratio. In other words, the vertical panels did not contribute to the lat-

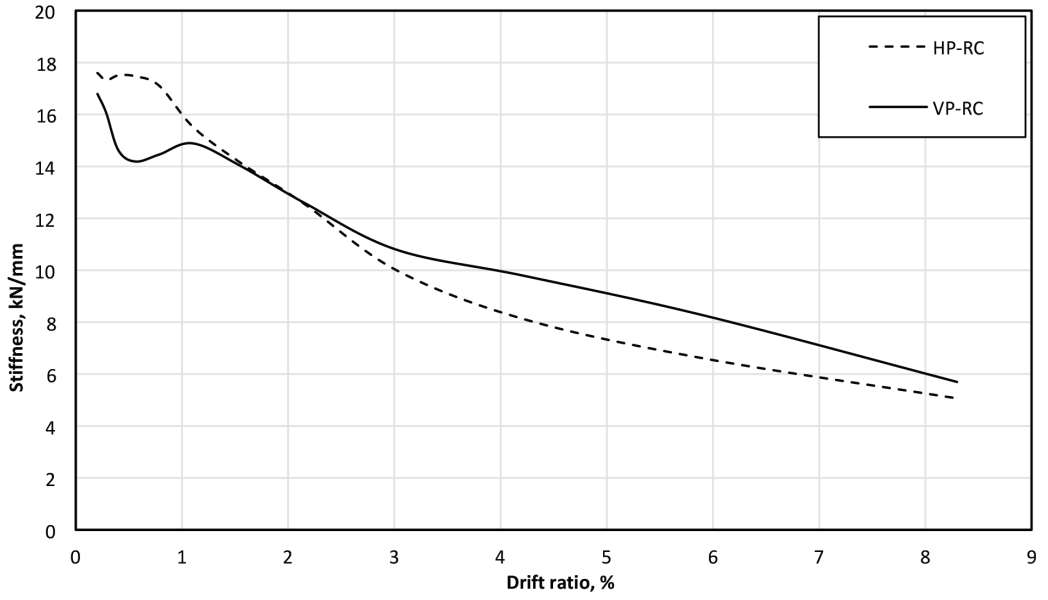

Figure 9. Stiffness-degrading curves. Note: HP-RC = horizontal panels in rigid connection frame; VP-RC = vertical panels in rigid connection frame. 1 kN/mm = 5.71 kip/in.

eral-load-resisting system until the 2% drift ratio was reached and it was only the steel frame that dissipated energy; as a result, plastic hinges formed at the base of the columns.

One of the major effects of placing the panels vertically is a larger stiffness with a drift ratio between 2% and 8% compared with horizontally placed panels. The larger stiffness is due to the rocking behavior of the vertical panels in the steel moment frame. VP-RC behaves as a braced frame with the vertical panels forming compression struts, whereas the horizontal panel placement shows a sliding behavior and has a smaller stiffness value at higher drift ratios. Stiffness degradation in both frames was the result of concrete crushing, separation of column components, loss of bond, and other factors, and the only difference was the orientation of panels.

Furthermore, VP-RC was better able to maintain sufficient strength at large deformations, which is known as ductility, compared with HP-RC. Ductile behavior prevents collapse in the event of excessive lateral loads that may convert all joints into plastic hinges.

In summary, the sliding behavior of specimen HP-RC showed more degradation of stiffness with the increase of drift ratio than VP-RC with its rocking behavior.

Energy dissipation

An important parameter in evaluating seismic performance of structural walls is their ability to dissipate energy when the structure is subjected to cyclic loads. Hollow-core units are assumed to be nonstructural walls in this paper; however, they must be able to dissipate energy reliably to improve the seismic behavior of the steel moment frame.

A convenient way to quantify energy-dissipation capacity is to determine the area under the load-displacement hysteresis loops. Using this method, both frames showed similar energy-dissipation capacity at lower drift ratios up to 2.5%. The pinching in hysteresis behavior of VP-RC at drift ratios of 2.5% to 4.5% caused by the gaps between panels and columns results in slightly lower energy dissipation compared with HP-RC.

At higher drift ratios, specimen VP-RC achieved approximately 10% higher energy-dissipation capacities compared with specimen HP-RC (**Fig. 10**). The differences in energy-dissipation behavior between specimens VP-RC and HP-RC are the result of rocking behavior, compression struts, and gradual closing of the gaps in VP-RC.

The energy dissipation for each specimen is similar for each individual cycle; however, a comparison between the two systems with similar strength, tested under the same cyclic loading protocol, indicated that specimen VP-RC, with its higher energy absorption, should exhibit superior performance, especially at higher drift ratios.

Equivalent viscous damping

Another way to quantify energy-dissipation capacity is in terms of damping. For specimens subjected to cyclic loading, the equivalent viscous damping ratio ξ_{eq} can be obtained from Eq. (1).[25]

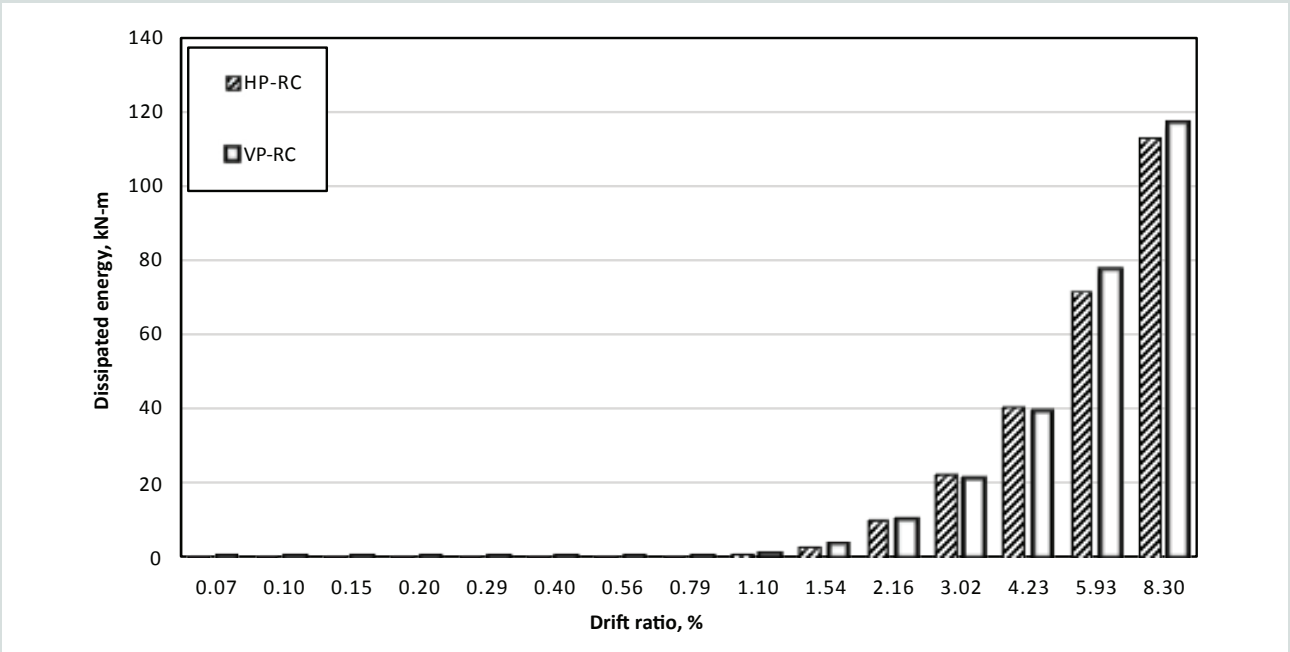

Figure 10. Energy dissipation compared with drift ratio. Note: HP-RC = horizontal panels in rigid connection frame; VP-RC = vertical panels in rigid connection frame. 1 kN-m = 8.85 kip-in.

$$\xi_{eq} = \frac{E_i}{4\pi E_e} \quad (1)$$

where

E_i = energy dissipated at cycle i

E_e = elastic strain energy stored in an equivalent linear elastic system when the maximum displacement is reached at cycle i

Figure 11 shows the equivalent viscous damping ratio for each specimen as a function of drift ratio. At a drift ratio of less than 0.5%, the damping ratio for specimen VP-RC was about four times the damping ratio for specimen HP-RC. The higher damping ratio for VP-RC was caused by the open gaps between panels and columns at this point in the testing, thus it is expected that the overall stiffness of the system was provided only by the steel frame members.

At a drift ratio of 1.24%, the damping ratio was the same for both specimens, and finally at the ultimate drift ratio, the damping ratio for specimen HP-RC was 0.27, while the damping ratio for specimen VP-RC was 0.23. At moderate and higher drift ratios, the viscous damping ratio for HP-RC increased with increased loading.

The equivalent viscous damping ratio for VP-RC increased as the drift ratio increased up to a drift ratio of 0.5%, after which the damping ratio decreased until a drift ratio of 1% was reached (Fig. 11). This trend was due to the gaps between the panels and columns that was explained previously. The distribution of plastic hinges in the steel frame and other damage to the system caused the dissipating energy to gradually increase starting from a drift ratio of 1%. As a result, the equivalent viscous damping ratio increased as drift ratio increased.

When comparing corresponding loops of the two hysteresis curves (Fig. 5) with similar energy dissipations but significant differences in peak loads, the equivalent viscous damping ratio is not a suitable parameter to assess the energy-dissipation capacity of specimens. This is due to the ratio calculation method described in Eq. (1).

Conclusion

This experimental study focused on the orientation of hollow-core wall panels in steel moment frames. The behavioral characteristics of the specimens were quantified with an emphasis on hysteretic energy dissipation, stiffness-degrading parameters, and failure modes.

The following conclusions are based on the test results presented in this paper:

- The VP-RC specimen had more panel damage than HP-RC had. The panel damage was defined as nonstructural damage.
- The stiffness of a steel moment frame can be significantly increased—while maintaining the same ductility level—when vertical hollow-core panels are used.
- HP-RC had more-significant steel frame damage than VP-RC. The steel moment frame damage was described as structural damage.

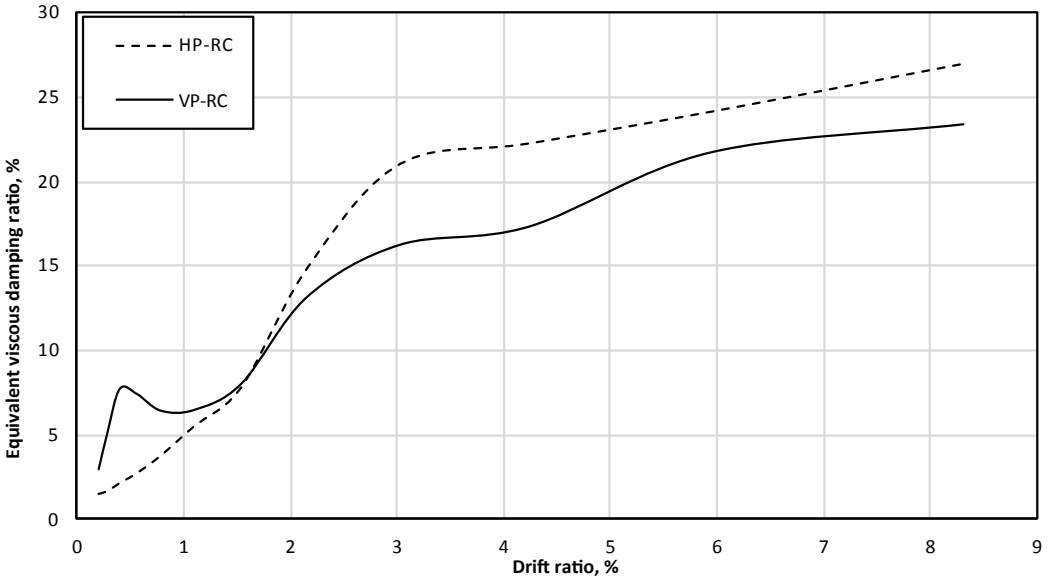

Figure 11. Equivalent viscous damping ratio. Note: HP-RC = horizontal panels in rigid connection frame; VP-RC = vertical panels in rigid connection frame.

- Apart from the similarity in energy-dissipation capacity, the steel moment frame with vertically placed hollow-core wall units had better overall performance than the steel moment frame with hollow-core wall units placed horizontally. The system with the vertically placed panels is considered to perform better because of the nonstructural nature of the damage to the panels and the ability of the rigid connections to resist higher lateral loads.

- The stiffness of the specimen with vertical hollow-core panels was greater than that of the specimen with horizontal hollow-core panels for drift ratios greater than 3%.

- The movement of the vertical panels in the steel moment frame was defined as rocking behavior, while sliding behavior best describes the horizontal panel movement within the steel moment frame. The formation of compression struts in the vertical panels had a considerable effect on the cyclic behavior of the steel frame.

This limited experimental work determined that vertical placement of hollow-core wall units is more effective and shows a better overall seismic performance of steel moment frames subjected to the large deformations caused by severe earthquakes.

References

1. Hamid, N. H., and John B. Mander. 2010. "Lateral Seismic Performance of Multipanel Precast Hollowcore Walls." *Journal of Structural Engineering* 136 (7): 795–804.

2. Hamid, N., and J. B. Mander. "Experimental Study on Bi-lateral Seismic Performance of Precast Hollow Core Wall Using Shaking Table." In *Proceedings of the 10th East Asia-Pacific Conference on Structural Engineering and Construction (EASEC-10), August 3–5, 2006, Bangkok, Thailand*. Bangkok, Thailand: Asian Institute of Technology.

3. Bull, D. K. 2000. *Guidelines for the Use of Structural Precast Concrete in Buildings*. Christchurch, New Zealand: University of Canterbury Centre for Advanced Engineering.

4. Palmer, Keith D., and Arturo E. Schultz. 2010. "Factors Affecting Web-Shear Capacity of Deep Hollow-Core Units." *PCI Journal* 55 (2): 123–146.

5. Palmer, Keith D., and Arturo E. Schultz. 2011. "Experimental Investigation of the Web-Shear Strength of Deep Hollow-Core Units." *PCI Journal* 56 (4): 83–104.

6. PCI Committee on Precast Sandwich Wall Panels. 2011. "State of the Art of Precast/Prestressed Concrete Sandwich Wall Panels: Second Edition." *PCI Journal* 56 (2): 131–176.

7. Building Seismic Safety Council. 2012. *NEHRP Recommended Seismic Provisions: Design Examples*. FEMA P-751. Washington, DC: Federal Emergency Management Agency.

8. Hawkins, Neil M., and S. K. Ghosh. 2006. "Shear Strength of Hollow-Core Slabs." *PCI Journal* 51 (1): 110–114.

9. Girhammar, Ulf Arne, and Matti Pajari. 2008. "Tests and Analysis on Shear Strength of Composite Slabs of Hollow Core Units and Concrete Topping." *Construction and Building Materials* 22 (8): 1708–1722.

10. Bertagnoli, Gabriele, and Giuseppe Mancini. 2009. "Failure Analysis of Hollow-Core Slabs Tested in Shear." *Structural Concrete* 10 (3): 139–152.

11. Pajari, Matti. 2009. "Web Shear Failure in Prestressed Hollow Core Slabs." *Journal of Structural Engineering* 42 (4): 83–104.

12. Cheng, Shaohong, and Xuefei Wang. 2010. "Impact of Interaction Between Adjacent Webs on the Shear Strength of Prestressed Concrete Hollow-Core Units." *PCI Journal* 55 (3): 46–63.

13. Rahman, M. K., M. H. Baluch, M. K. Said, and M. A. Shazali. 2012. "Flexural and Shear Strength of Prestressed Precast Hollow-Core Slabs." *Arabian Journal for Science and Engineering* 37 (2): 443–455.

14. Cuenca, E., and P. Serna. 2013. "Failure Modes and Shear Design of Prestressed Hollow Core Slabs Made of Fiber-Reinforced Concrete." *Composites Part B: Engineering* 45 (1): 952–964.

15. Brunesi, E., D. Bolognini, and R. Nascimbene. 2015. "Evaluation of the Shear Capacity of Precast-Prestressed Hollow Core Slabs: Numerical and Experimental Comparisons." *Materials and Structures* 48 (5): 1503–1521.

16. Perez, Felipe J., Stephen Pessiki, and Richard Sause. 2004. "Seismic Design of Unbonded Post-Tensioned Precast Concrete Walls with Vertical Joint Connectors." *PCI Journal* 49 (1): 58–79.

17. Holden, Tony, Jose Restrepo, and John B. Mander. 2003. "Seismic Performance of Precast Reinforced and Prestressed Concrete Walls." *Journal of Structural Engineering* 129 (3): 286–296.

18. AISC (American Institute of Steel Construction). 2010. *Prequalified Connections for Special and Intermediate Steel Moment Frames for Seismic Applications*. With supplement 1. ANSI/AISC 358-10. Chicago, IL: AISC.

19. ASTM Subcommittee E28.04. 2009. *Standard Test Methods for Tension Testing of Metallic Materials*. ASTM E8/E8M-09. West Conshohocken, PA: ASTM International.

20. ASTM Subcommittee C09.61. 2001. *Standard Test Method for Compressive Strength of Cylindrical Concrete Specimens*. ASTM C39/C39M-01. West Conshohocken, PA: ASTM International.

21. ASTM Subcommittee A01.05. 2012. *Standard Specification for Steel Strand, Uncoated Seven-Wire for Prestressed Concrete*. ASTM A416/A416M-12. West Conshohocken, PA: ASTM International.

22. FEMA (Federal Emergency Management Agency). 2007. *Interim Testing Protocols for Determining the Seismic Performance Characteristics of Structural and Nonstructural Components*. FEMA 461. Washington, DC: FEMA.

23. FEMA. 2005. *Improvement of Nonlinear Static Seismic Analysis Procedures*. FEMA 440. Washington, DC: FEMA.

24. ASCE (American Society of Civil Engineers). 2013. *Seismic Evaluation and Retrofit of Existing Buildings*. ASCE/SEI 41-13. Reston, VA: ASCE.

25. Priestley, M. J. N., F. Seible, and G. M. Calvi. 1996. *Seismic Design and Retrofit of Bridges*. New York, NY: John Wiley and Sons.

Notation

E = modulus of elasticity of steel

E_e = elastic strain energy stored in an equivalent linear elastic system when the maximum displacement is reached at cycle i

E_i = energy dissipated at cycle i

f_c' = concrete compressive strength

F_u = ultimate tensile strength of steel

F_y = yield strength of steel

i = cycle number

K_e = initial stiffness of the specimen

V = applied load

V_d = applied load at ultimate strength

V_y = applied load at yielding

δ = drift ratio

δ_d = drift ratio at ultimate strength

δ_y = drift ratio at yielding

Δ = lateral displacement

Δ_d = lateral displacement at ultimate strength

Δ_y = lateral displacement at yielding

ξ_{eq} = equivalent viscous damping ratio

About the authors

Mehdi Nazarpour is a PhD candidate in the Department of Structural Engineering at the International Institute of Earthquake Engineering and Seismology (IIEES) in Tehran, Iran. The main fields of his research include precast concrete wall panels; high-strength concrete; squat reinforced concrete shear walls; and repair, rehabilitation, and retrofitting of structures.

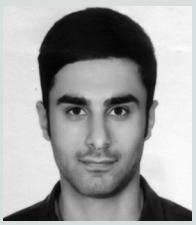

Parsa Monfaredi is a structural engineer in the Department of Structural Engineering at IIEES, where he also received his master's degree in 2016 in the field of precast concrete hollow-core wall panels.

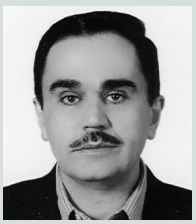

Abdoreza S. Moghadam received his BSc in civil engineering in 1987 and his MSc in structural engineering in 1991, both from Tehran University in Iran, and his PhD in earthquake engineering in 1999 from McMaster University in Hamilton, ON, Canada. His research interests include earthquake engineering, evaluation and design of tall buildings, development of building codes, seismic retrofitting of structures, and the effects of three-dimensional modeling in the evaluation and design of buildings. He is currently an associate professor at IIEES.

Abstract

Hollow-core precast concrete panels are widely used as nonstructural wall units in steel structures. This experimental research evaluated the lateral seismic performance of hollow-core panels placed in a steel moment frame. This paper discusses the effects of the orientation of the hollow-core panels that were reinforced with two layers of high-strength, bonded pretensioning strands for lateral resistance. A half-scale steel moment frame with two hollow-core panels placed horizontally was tested with cyclic lateral loading and a constant axial load. An identical frame with two panels placed vertically was tested in the same manner. The test results indicated that vertical placement of hollow-core wall units was more effective in resisting lateral loading and a higher load-bearing capacity was achieved, as well as better flexibility and ductility compared with panels placed horizontally. The damage sustained by the system with the vertical panels was considered to be nonstructural damage, which is more desirable than structural steel frame damage. The vertical placement of hollow-core wall units controlled nonstructural damage, improved the seismic behavior of the steel moment frame at high seismic forces and resisted higher lateral loads. The movement of the hollow-core panels in the steel moment frame was observed with the vertical panels rocking within the frame and the horizontal panels sliding against each other.

Keywords

Hollow-core, multipanel hollow-core wall, nonstructural damage, quasi-static cyclic loading, rocking mechanism, seismic behavior.

Review policy

This paper was reviewed in accordance with the Precast/Prestressed Concrete Institute's peer-review process.

Reader comments

Please address any reader comments to *PCI Journal* editor-in-chief Emily Lorenz at elorenz@pci.org or Precast/Prestressed Concrete Institute, c/o *PCI Journal*, 200 W. Adams St., Suite 2100, Chicago, IL 60606.